JOURNAL OF SOLID STATE CHEMISTRY 58, 14–28 (1985)

Variations on the Theme of Closest Packing: The Structural Chemistry of Barium Titanate Compounds

EKKEHART TILLMANNS AND WOLFGANG HOFMEISTER

Institut für Geowissenschaften, Postfach 3980, Universität Mainz, D-6500 Mainz, Bundesrepublik Deutschland

AND WERNER H. BAUR

Department of Geological Sciences, Box 4348, University of Illinois at Chicago, Chicago, Illinois 60680

Received June 5, 1984; in revised form September 24, 1984

The crystal structures of most barium titanates can be described as hexagonal closest packings consisting of atoms of Ba and O and of vacancies between them. The pseudohexagonal cell constants of these compounds are close to the ideal hexagonal values. The most common stacking is the six-layer sequence $(hcc)_2$. The mean diameter of a closest packed particle in these packings is 2.85 Å, while the mean thickness of a layer is 2.33 Å. The recognition of this closest packing principle has been helpful in the solution of many of the crystal structures of this group. With the exception of $BaTi_4O_9$, all the barium titanates which are usually classified as tunnel structures or Wadsley–Andersson phases can be described as cubic closest packings. The deviations of the pseudocubic phases from the ideal cubic values are larger than in the pseudohexagonal cases. A few of the barium titanates are related to the so-called 3.0-Å phases based on the rutile-type octahedral chain. These structures are characterized by having two almost closest packed corrugated layers at right angles to each other. The structures of a number of compounds in which the Ti^{4+} atoms are replaced partly by Ti^{3+}, Al, Pt^{4+}, or Li are based on principles similar to those of the barium titanates proper. The mean Ti–O distances in the coordination octahedra of the barium titanates depend strongly on the distortions of the octahedra.

Introduction

Some of the chemical compounds in the system $BaO–TiO_2$ are of importance in materials science because they have interesting properties, such as ferroelectricity, or else they have attractive dielectric properties at microwave frequencies. For the same reasons they are interesting to study from the standpoint of basic research: they give a chance to correlate crystalline structure with physical properties. In the last 35 years many papers have appeared in which measurements of their physical properties, their phase relations, and their crystal structures have been reported.

The subsolidus phase relations in the system $BaTiO_3–TiO_2$ were studied by Statton (*1*) and by Rase and Roy (*2*), while the phase equilibria in the TiO_2–rich part of the system were investigated by Negas *et al.* (*3*) and by O'Bryan and Thomson (*4*). With the determination of the crystal structure of $Ba_2Ti_9O_{20}$ (*5*), all the structures of the stable compounds in the system $BaO–TiO_2$ are known: Ba_2TiO_4 (*6*, *7*), cubic $BaTiO_3$ (*8*),

0022-4596/85 $3.00

hexagonal $BaTiO_3$ (*9*) (however it is doubtful that hexagonal $BaTiO_3$ can be prepared without stabilization by the addition of small amounts of other octahedral cations, for instance, Pt, see (*10*)), $Ba_6Ti_{17}O_{40}$ (*11, 12*), $Ba_4Ti_{13}O_{30}$ (*13*), $BaTi_4O_9$ (*12, 14, 15*), $Ba_2Ti_9O_{20}$ (*5*), and rutile (TiO_2 (*16, 17*)). In addition, the structures of several barium titanates which are metastable or occur as intermediate reaction products have been solved: $BaTi_2O_5$ (*18*), $BaTi_5O_{11}$ (*19*), and $BaTi_6O_{13}$ (*20*). For comparative purposes we have also included data for brookite (*21, 22*), anatase (*23*), TiO_2-II (a high pressure modification of the α-PbO_2 type, see (*24*)) and TiO_2(B) (a 4.0-Å tunnel structure type, see (*25*)). The crystal structure of TiO_2(B) has not been refined; however, it is known to be isostructural to the corresponding vanadium compound, VO_2(B) (*26*). Other compounds reported to exist are $Ba_2Ti_3O_8$ (*27*) and $BaTi_3O_7$ (*28*). Most likely the former actually was tetragonal $BaTiO_3$ and the latter $Ba_4Ti_{13}O_{30}$; however, the corresponding lead compound ($PbTi_3O_7$) has been structurally characterized (*29*). The composition $Ba_2Ti_5O_{12}$ was reported by Jonker and Kwestroo (*30*) to occur in this system. They probably observed the $Ba_6Ti_{17}O_{40}$ compound, but did not assign the correct composition to it (*3*).

Some compounds exhibit slight chemical variations when compared with the barium titanates, even though their structural characteristics are similar to them. In some of them the Ti positions are partly vacant ($Ba_2Ti_{5.5}O_{13}$ (*31*) and $Ba_2Ti_{9.25}Li_3O_{22}$ (*32*)), in others the Ti^{4+} atoms are partly substituted by formally trivalent atoms such as Ti^{3+} or Al ($Ba_2Ti_2^{3+}Ti_4^{4+}O_{13}$ (*33*), $BaTi_6^{4+}Ti_2^{3+}O_{16}$ (*34*), and $Ba_4Ti_{10}Al_2O_{27}$ (*35*)), in others the octahedral sites are partially occupied by other tetravalent elements such as Pt (as in $Ba(Ti,Pt)O_3$ and $Ba_4(Ti,Pt)_2PtO_{10}$ (*10*)), or else there are additional octahedral cations present as in $Ba_2Ti_{9.25}Li_3O_{22}$ (*32*).

Most of the barium titanates can be described as closest packings of Ba and O atoms, in which some of the octahedral O_6 interstices are occupied by Ti atoms. All the barium titanates can also be described as variously connected assemblages of TiO_6 octahedra. Such descriptions are most useful either when we follow a scheme in which the long axes of the octahedra are emphasized (the 4.0-Å axes, as in the Wadsley–Andersson-type phases, also called tunnel structures) or when we stress the columns of edge-shared octahedra with an identity period of 3.0 Å as they are known from rutile and similar structures (the 3.0-Å-type structures).

This work is limited to compounds in the $BaTiO_3$–TiO_2 system (i.e., the ratio Ba/Ti is less than 1); thus Ba_2TiO_4 and BaO are not covered. But we included compounds in which Ti^{4+} is partly replaced by vacancies, Pt, Al, or Ti^{3+}, as long as they are based on the same principles as the barium titanates. For all of these compounds crystal data and references are given in Table I.

Coordination Numbers and Polyhedral Shapes

Titanium occurs in octahedral 6-coordination against oxygen in all barium titanates except in Ba_2TiO_4 where it is 4-coordinated. Five-coordinated Ti has been observed (*36*), but not in any barium titanate.

The Ba atoms are surrounded by 10 to 12 O atoms. When in 12-coordination the oxygen atoms are arranged on the vertices of a cuboctahedron or of a hexagonally 12-coordinated polyhedron, depending on the location of the Ba atom in the center of a closest packed sequence which is either cubic (ABC or c) or hexagonal (ABA or h). The most common coordination of barium in these compounds is an 11-coordination generated by an oxygen vacancy in one of the cubic closest packed oxygen atom sites, that is, one of the vertices of the cuboctahe-

TABLE I

COMPOUNDS COVERED HERE

Compound	Type	Space group	a	b	c	α	β	γ	V	Z	D_x	O/Oc	Ba/Oc	Ref.
$Ba_4(Ti,Pt)_2PtO_{10}$	R	*Cmca*	5.783(1)	13.368(2)	13.129(1)	90	90	90	1015.0	4	6.73	3.33	1.33	(*10*)
$Ba(Ti,Pt)O_3$	C	$P6_3/mmc$	5.723(1)	5.723(1)	14.023(1)	90	90	120	397.8	6	6.28	3.00	1.00	(*10*)
$BaTiO_3$	C	*Pm3m*	4.0092(5)	4.0092(5)	4.0092(5)	90	90	90	64.4	1	3.97	3.00	1.00	(*8*)
$BaTi_2O_5$	W	*A2/m*	9.409(3)	3.932(1)	16.907(5)	90	103.08(2)	90	609.3	6	5.12	2.50	0.50	(*18*)
$Ba_6Ti_{17}O_{40}$	C	*C2/c*	9.887(1)	17.097(2)	18.918(2)	90	98.72(2)	90	3160.9	4	4.79	2.35	0.35	(*12*)
$Ba_2Ti_{5.5}O_{13}$	W	*C2/m*	15.160(4)	3.893(1)	9.093(2)	90	98.6(1)	90	530.6	2	4.67	2.17	0.33	(*31*)
$Ba_2Ti_2^{3+}Ti_4^{4+}O_{13}$	W	*C2/m*	15.004	3.953	9.085	90	98.01	90	533.6	2	4.79	2.17	0.33	(*68*)
$Ba_4Ti_{10}Al_2O_{27}$	C	*C2/m*	19.737	11.349	9.837	90	109.4	90	2078.3	4	4.84	2.25	0.33	(*35*)
$Ba_4Ti_{13}O_{30}$	C	*Cmca*	17.062(5)	9.862(3)	14.051(4)	90	90	90	2364.3	4	4.64	2.31	0.31	(*13*)
$BaTi_4O_9$	W	*Pmmn*	14.527(2)	3.794(1)	6.293(1)	90	90	90	346.8	2	4.53	2.25	0.25	(*12*)
$BaTi_4O_9$(hypoth.)	W	*I2/m*	14.77	3.79	6.29	90	100.3	90	346.4	2	4.53	2.25	0.25	(*56*)
$Ba_2Ti_9O_{20}$	C	$P\bar{1}$	7.471(1)	14.081(1)	14.344(2)	89.94(2)	79.43(2)	84.45(2)	1476.2	4	4.62	2.22	0.22	(*5*)
$Ba_2Ti_{9.25}Li_3O_{22}$	C	*Pmcn*	5.808(5)	9.931(1)	14.025(1)	90	90	90	809.0	2	4.48	2.20	0.20	(*32*)
$BaTi_5O_{11}$	C	$P2_1/n$	7.67(2)	14.02(3)	7.52(2)	90	98.33(7)	90	800.1	4	4.58	2.20	0.20	(*19*)
$BaTi_6O_{13}$	C	$P\bar{1}$	7.510(2)	9.852(3)	7.461(2)	105.38(2)	118.90(2)	72.58(2)	456.3	2	4.61	2.17	0.17	(*20*)
$BaTi_6^{4+}Ti_2^{3+}O_{16}$	R	*C2*	14.209	2.971	9.981	90	133.5	90	305.6	1	4.22	2.00	0.13	(*34*)
$BaTi_6Al_2O_{16}$	R	*I4/m*	10.039(1)	10.039(1)	2.943(1)	90	90	90	296.6	1	4.23	2.00	0.13	(*69*)
TiO_2-II	C	*Pbcn*	4.515(6)	5.497(5)	4.939(5)	90	90	90	122.6	4	4.32	2.00	0.00	(*24*)
Rutile	R	$P4_2/mnm$	4.5941(1)	4.5941(1)	2.9589(1)	90	90	90	62.5	2	4.25	2.00	0.00	(*16*)
Brookite	C	*Pbca*	9.174(2)	5.449(2)	5.138(2)	90	90	90	256.8	8	4.13	2.00	0.00	(*22*)
Anatase	C	$I4_1/amd$	3.7842(1)	3.7842(1)	9.515(2)	90	90	90	136.3	4	3.89	2.00	0.00	(*23*)
TiO_2(B)	W	*C2/m*	12.163(5)	3.735(2)	6.513(2)	90	107.29(5)	90	282.5	8	3.76	2.00	0.00	(*25*)

Note. Type C refers to structures which are most conveniently described as closest packings of barium and oxygen atoms, type W to Wadsley–Andersson phases, and type R to rutile-related 3.0-Å phases. The value O/Oc gives the ratio between the number of oxygen atoms to occupied octahedral sites, while Ba/Oc is the ratio of barium atoms to occupied octahedral sites. The compounds are sorted according to decreasing values of Ba/Oc.

dron is removed. In $Ba_4(Ti,Pt)_2PtO_{10}$ the 11-coordination is formed by removing one edge from a hexagonal 12-coordination and replacing it at its midpoint by a vertex. Neither of these 11-coordinations corresponds to the 11-coordinated equivalent packing observed in rutile and related compounds (*17*). Ten-coordination occurs only twice: in the case of $BaTi_4O_9$ as a distorted pentagonal prism, and in $Ba_4(Ti,Pt)_2PtO_{10}$ as a hexagonal 12-coordination with an edge removed.

The O atoms are coordinated by three to six cations with the mean coordination number increasing in individual barium titanates as the Ba : Ti ratio increases (Fig. 1). Two-coordinated oxygen occurs only in TiO_2(B) (*25*). The mean cation coordination number of all 166 crystallographically unique oxygen atoms in the sample is 4.11. Each oxygen atom can be coordinated by one to four Ti atoms and can have between zero and five Ba contacts. Extreme values are rare: the only case of an oxygen atom with five Ba neighbors occurs in $Ba_4(Ti,Pt)_2PtO_{10}$.

Polyhedral Connections

Since the ratio of O atoms to octahedrally coordinated cations ranges from 3.33 to 2.00 (Table I) we must expect widespread sharing of octahedral elements between the coordination octahedra in these compounds. Only if the ratio were equal to or greater than 6 could we expect isolated octahedra. Complete octahedral stuffings of cubic and hexagonal closest packings have differently connected coordination octahedra: in the NaCl type there are three shared corners and six shared edges per asymmetric unit, while in the NiAs type there are six shared corners, three shared edges, and one shared face. Shared octahedral faces cannot occur in barium titanates derived from cubic closest packing. Moreover, they are also rare in those compounds which contain hexagonal sequences. There is one shared octahedral face per asymmetric unit in $Ba_6Ti_{17}O_{40}$, $BaTi_6O_{13}$, $Ba_4Ti_{10}Al_2O_{27}$, $Ba(Ti,Pt)O_3$, and $Ba_4(Ti,Pt)_2PtO_{10}$. This list includes the two Pt-containing compounds in our sample. Apparently the barium titanates proper avoid shared octahedral faces. In contrast shared octahedral faces are the rule in the hexagonal perovskite variants of other transition elements: $BaNiO_3$ (*37*), $BaCrO_3$ (*38*), and many more. This face sharing is quite common for Pt^{4+}-containing compounds (*39*); thus it is not surprising that $Ba(Ti,Pt)O_3$ and $Ba_4(Ti,Pt)_2PtO_{10}$ display shared octahedral faces.

The polyhedra around the Ba atoms share vertices, edges, and faces with each other, much as the TiO_6 octahedra do. The most interesting relationship occurs when a space is available between two cuboctahedrally coordinated Ba atoms for a closest packed oxygen atom. An O atom here would provide a common corner between the Ba cuboctahedra, but in fact it is absent. Consequently there are two 11-coordinated Ba atoms present for each vacant oxygen atom site. The Ba–Ba distance is then about 5.0 Å, much shorter than the approximately 6.0 Å observed when there is a common corner.

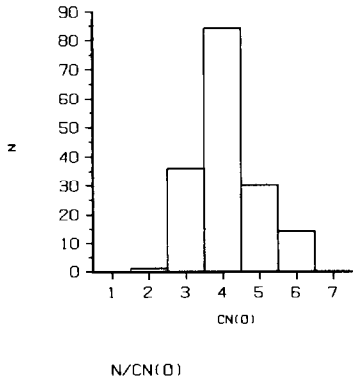

FIG. 1. Histogram of the coordination numbers of the oxygen atoms in the barium titanates and TiO_2 polymorphs.

Interatomic distances

The mean Ba–O bond lengths in the various Ba coordination polyhedra do not show a clear dependence on coordination number. The mean value of this distance Ba–O for 24 BaO_{10}, BaO_{11}, and BaO_{12} polyhedra is 2.915 Å (this omits $BaTi_6Al_2O_{16}$ and $BaTi_6^{4+}Ti_2^{3+}O_{16}$, where the Ba positions are half occupied). The mean distances range from 2.84 to 2.97 Å; the individual distances Ba–O range from 2.65 to 3.35 Å (see Figs. 2 and 3).

The mean of 58 average octahedral Ti^{4+}–O distances is 1.976 Å in the 10 Ba titanates. This is longer than the mean Ti–O distance of 1.958 Å found in the four refined TiO_2 modifications. The range of all 62 distances is from 1.942 to 2.020 Å (Fig. 4). The lengthening of the mean distances is most likely due to polyhedral distortion as discussed for the cases of octahedral Nb^{5+}–O and Mo^{6+}–O by Shannon (*40*). Octahedral distortion is defined as (*40*):

$$\Delta = 1/6\Sigma((R_i - R_m)/R_m)^2 \qquad (1)$$

where R_i is an individual cation–oxygen distance and R_m is a mean cation–oxygen distance in an octahedron. In addition the bond lengths around the Ti atoms in our sample are influenced by statistical occupations of the Ti sites by vacancies, Ti^{3+}, Al, or Pt. We increased our sample of mean octahedral Ti–O distances from the barium titanates by using the mean Ti–O bond lengths of the TiO_2 polymorphs, $PbTi_3O_7$ (*29*), $Na_{16}Ti_{10}O_{28}$ (*42*), $(Y,TR)_4(F,OH)_6TiO[SiO_4]_2$ (*43*), and $K_2Ti_6O_{13}$ (*44*) as well as those from several mixed Ti^{3+}, Ti^{4+} oxides, namely, Ti_2O_3 (*45*), Ti_3O_5 (*46*), Ti_4O_7 (*47*), Ti_5O_9 (*48*), and Ti_nO_{2n-1} ($4 \leq n \leq 9$) (*49, 50*). The distortion indices Δ and the Ti^{3+} and vacancy contents of the octahedral sites can be used as independent variables in a regression calculation, which gives us estimates for the mean octahedral bond lengths to the O atoms around the Ti sites. This equation can be used to predict $(Ti–O)_{mean}$ distances for different Δ values, vacancy (Vac), and Ti^{3+} contents of the coordination octahedra:

$$(Ti–O)_{mean} = [1.962(2) + 4.73(44)\Delta + 0.077(5)Ti^{3+} + 0.195(33)Vac]\ Å. \qquad (2)$$

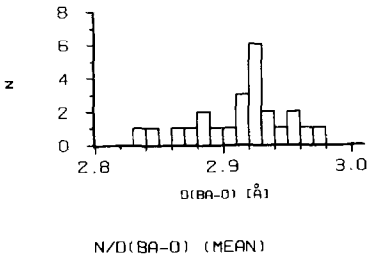

FIG. 2. Histogram of the mean Ba–O distances in the barium titanates.

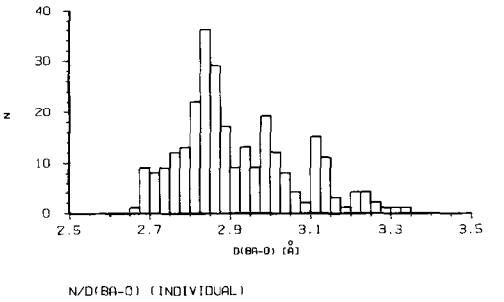

FIG. 3. Histogram of the individual Ba–O distances in the barium titanates.

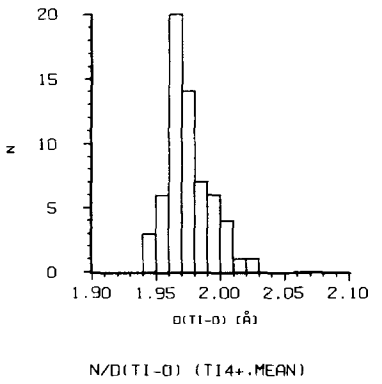

FIG. 4. Histogram of the mean Ti–O distances in the barium titanates and the modifications of TiO_2.

The number and the quality of the bond length data involving statistical occupations by Pt and Al did not allow their inclusion in the regression calculations. Equation (2) explains 67% of the variation in the 145 mean Ti–O bond lengths used in the regression, with a mean deviation between observation and estimate of 0.009 Å. The independent variables are significant contributors at the 99.99% level (Fig. 5). The intercept indicates that a pure Ti^{4+} in octahedral coordination in an undistorted oxygen atom environment should have a $(Ti–O)_{mean}$ value of 1.962 Å. The radii of Ti^{4+} and Ti^{3+} in octahedral coordination are given as 0.605 and 0.670 Å, respectively (*40*). The difference of 0.065 Å is similar to

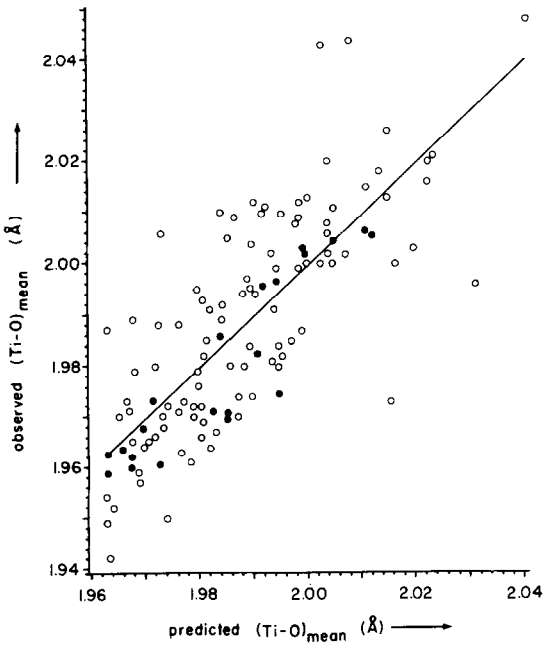

FIG. 5. Scatter plot of mean Ti–O distances in the barium titanates and the TiO_2 polymorphs versus the predicted mean distances Ti–O calculated from the regression equation including the dependence on distortion and Ti^{3+} and vacancy contents. The line is the 45° line on which the points should fall if the agreement were perfect. Single points are shown as open circles; multiple, unresolved points as filled circles. The same convention is used in Figs. 7, 8, and 16.

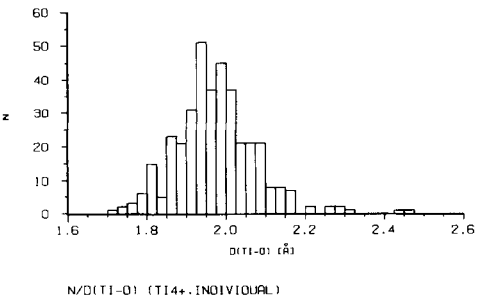

FIG. 6. Histogram of the individual Ti–O distances in the barium titanates and the TiO_2 modifications.

the slope of 0.077 for the Ti^{3+} content that we observed. The slope of the vacancy (partial occupancy) contribution is positive, as observed by Shannon (*40*) for partial occupancies by Li, Na, and Ag ions.

The large spread in individual Ti–O distances (from 1.723 to 2.465 Å, see Fig. 6) is explainable largely by the differences in bond strengths (*51*) received by the O atoms. As shown before (*52*) bond lengths in ionic or partly ionic structures can be predicted by empirical relations of the form

$$d(A–X)_{ind.} = [d(A–X)_{mean} + b\Delta p(X)]\text{Å}, \quad (3)$$

where $d(A–X)_{mean}$ and b are empirically derived values for the mean bond lengths and the slopes of the dependence of the individual bond lengths $d(A–X)_{ind.}$ on $p(X)$ for given pairs of A and X in a given coordination. Here $\Delta p(X)$ is the difference between the individual $p(X)$ and the mean $p(X)$ for the coordination polyhedron:

$$\Delta p(X) = p(X)_{ind.} - p(X)_{mean}. \quad (4)$$

A regression calculation using 354 $(Ti–O)_{ind.}$ from the barium titanates and the TiO_2 polymorphs gave

$$(Ti–O)_{ind.} = [1.973(4) + 0.260(14)\Delta p(O)]\ \text{Å}. \quad (5)$$

This equation explains 47% of the variation in $(Ti–O)_{ind.}$ and variable b is significant at the 99.99% level (Fig. 7). The values given

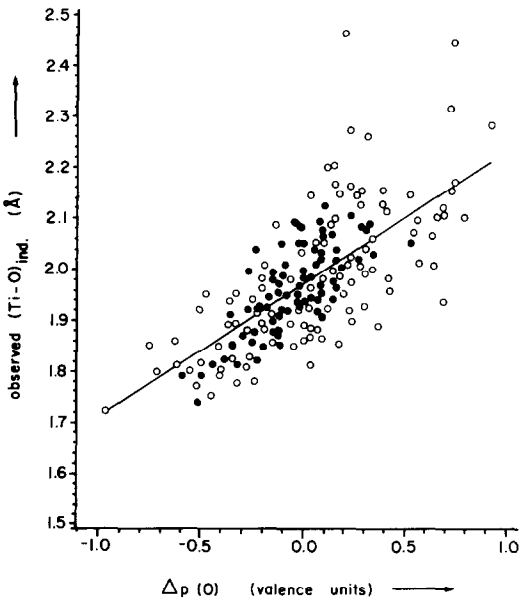

FIG. 7. Scatter plot of the individual Ti–O distances against bond strength deviations. The regression line has been entered.

here for the intercept and the slope are more reliable than those given before (*53*).

The agreement between observation and prediction is better ($r^2 = 0.86$) if we use the averages of the Ti–O bond lengths around each individual oxygen atom in a regression calculation on $p(O)$ itself instead of using the individual Ti–O distances (Fig. 8):

$$(O\text{–}Ti)_{mean} = [1.484(19) + 0.236(9)p(O)]\ \text{Å}. \quad (6)$$

The slopes in Eqs. (5) and (6) are equal within two pooled estimated standard deviations.

In the method of Brown and Shannon (*54*) one does not look at individual bond lengths as in Eq. (5), but compares the sums of bond strengths at both cation and anion sites. Therefore one would expect that these summations would give very good fits. In their method relationships of the form

$$s = (R/R_0)^{-N} \quad (7)$$

are used, where bond strength s, bond length R, R_0, and N are fitted parameters. The sum of the bond strengths around each ion should result in a value equal to the valence of the ion. However, even when using the improved parameter values of Wu and Brown (*7*) and Brown and Wu (*55*) the fit for the Ba titanates is poor. The bond strength sums around oxygen vary from 1.77 to 2.42 (instead of 2), around Ba from 2.03 to 2.32 (instead of 2), and around Ti from 4.01 to 4.75 (instead of 4). Apparently the reasonable fit observed for many other structures does not hold true for the barium titanates.

Close-Packed Arrangements of Ba and O Atoms

The group of barium titanates in which the closest packing of Ba and O atoms is

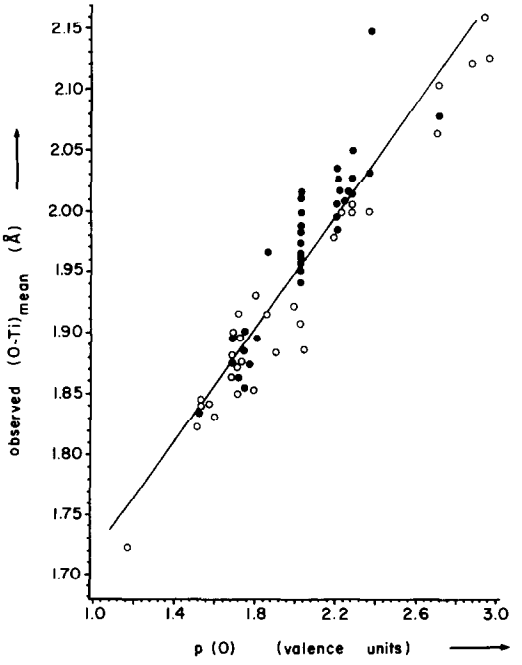

FIG. 8. Scatter plot of the mean O–Ti distances against predicted mean distances based on the dependence on bond strengths. The regression line is entered.

most clearly evident comprises the crystal structures of $Ba_6Ti_{17}O_{40}$, $Ba_4Ti_{10}Al_2O_{27}$, $Ba_4Ti_{13}O_{30}$, $Ba_2Ti_{9.25}Li_3O_{22}$, $Ba_2Ti_9O_{20}$, $BaTi_5O_{11}$, $BaTi_6O_{13}$, and both modifications of $BaTiO_3$. This structural feature is often reflected in the macroscopic shape of the crystals which in the case of hexagonal $BaTiO_3$, $Ba_6Ti_{17}O_{40}$, $BaTi_5O_{11}$, and $BaTi_6O_{13}$ grow as plates parallel to the closest packed layers. With the exception of $BaTi_4O_9$, however, the TiO_6 octahedra in all the other barium titanate structures are also oriented with at least one pair of their faces parallel to each other, so that they too can be represented by closest packed layers of Ba and O atoms, as shown in Fig. 9 for $BaTi_{5.5}O_{13}$. However, even in $BaTi_4O_9$ a close relationship to this principle has been shown by Hervieu *et al.* (*56*). They describe the orthorhombic structure of $BaTi_4O_9$ as a hypothetical twin of two monoclinic individuals containing TiO_6 octahedra with parallel faces. The observed and the hypothetical structures of $BaTi_4O_9$ are juxtaposed in Figs. 10 and 11. Table II gives pseudohexagonal and, where applicable, pseudocubic unit cells for the barium titanates. The pseudo character of these cells is expressed in their conforming to either cubic or hexagonal closest packing patterns as long as we regard oxygen atoms, barium atoms, and vacancies in the closest packings as equivalent to each other. Once they are distinguished and some of the octahedral inter-

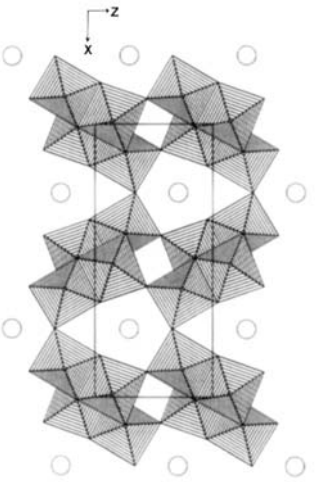

FIG. 10. Projection of $BaTi_4O_9$ parallel to [010]. This is the only structure among the barium titanates which cannot be described as a closest packing of barium and oxygen atoms, because the coordination octahedra around the titanium atoms are not oriented parallel to each other. The circles represent the barium atoms.

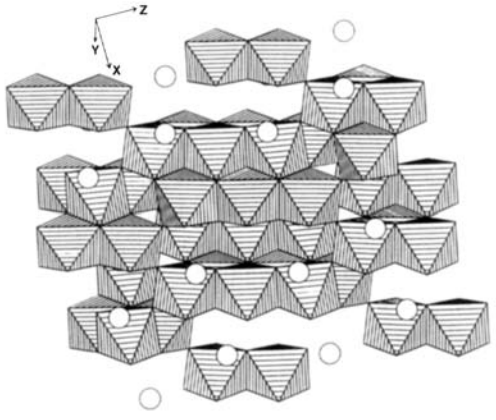

FIG. 9. Projection of the crystal structure of $Ba_2Ti_{5.5}O_{13}$ parallel to one of the four pseudocubic closest packed directions. The like orientation of all the coordination polyhedra is clearly visible.

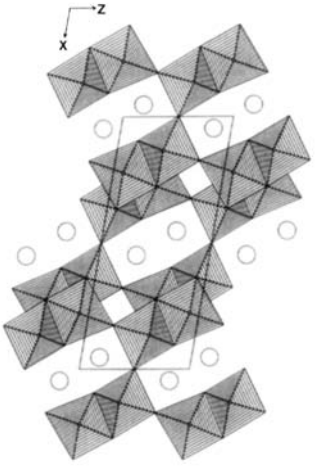

FIG. 11. Projection of the hypothetical $BaTi_4O_9$ structure parallel to [010]. All titanium coordination octahedra are parallel to each other. This structure is pseudocubic.

TABLE II

PSEUDOHEXAGONAL AND PSEUDOCUBIC CELLS OF CLOSEST PACKED AND WADSLEY–ANDERSSON-TYPE BARIUM TITANATE PHASES

Compound	Pseudocell in terms of original cell	Number of layers	Stacking sequence	a	b	c	α	β	γ	Diam. atom	Layer width
$Ba(Ti,Pt)O_3$	1 0 0 / 0 1 0 / 0 0 1	6	$(hcc)_2$	5.72	5.72	14.02	90	90	120	2.86	2.34
$BaTiO_3$	1 −1 0 / −1 0 1 / 1 1 1	3	$(c)_3$	5.67	5.67	6.94	90	90	120	2.84	2.32
$Ba_6Ti_{17}O_{40}$	1.5 −0.5 0 / 0 1 0 / 1 0 3	24	$(hcch)_6$	17.12	17.10	56.11	90	88.9	120.0	2.85	2.34
$Ba_4Ti_{13}O_{30}$	1 0 0 / −0.5 1.5 0 / 0 0 1	6	$(hcc)_2$	17.06	17.08	14.05	90	90	120.0	2.84	2.34
$Ba_2Ti_9O_{20}$	0 0 3 / 5 0 −2 / −2 9 0	54	$(hhc)_{18}$	43.03	42.72	126.16	90.3	91.2	120.7	2.86	2.34
$Ba_2Ti_{9.25}Li_3O_{22}$	1 1 0 / −2 0 0 / 0 0 1	6	$(hcc)_2$	11.50	11.62	14.03	90	90	120.3	2.89	2.34
$BaTi_5O_{11}$	−3 0 −1 / 1 0 3 / 0 1 0	6	$(hcc)_2$	23.15	22.75	14.02	90	90	119.9	2.87	2.34
$BaTi_6O_{13}$	1 0 3 / 2 0 −1 / −1 4 1	16	$(h)_{16}$	19.87	19.74	37.23	89.6	88.5	118.9	2.83	2.33
TiO_2-II	0 −1 2 / 0 2 0 / 1 0 0	2	$(h)_2$	11.30	10.99	4.52	90	90	119.1	2.79	2.26
Brookite	0 −1 2 / 0 2 0 / 1 0 0	4	$(hc)_2$	11.63	10.90	9.17	90	90	117.9	2.82	2.29
Anatase	2 −2 0 / −2 0 1 / 2 2 1	6	$(c)_6$	10.70	12.16	14.32	79.0	90	116.1	2.86	2.39
$BaTi_2O_5$	4 0 1 / 0 9 0 / −1 0 2	27	$(c)_{27}$	37.61	35.39	37.09	90	91.4	90	2.88	2.35
$Ba_2Ti_{5.5}O_{13}$	2 0 2 / 0 8 0 / −1 0 3	24	$(c)_{24}$	32.94	31.14	33.13	90	92.4	90	2.86	2.34
$Ba_2Ti_{12}^{3+}Ti_4^{4+}O_{13}$	2 0 2 / 0 8 0 / −1 0 3	24	$(c)_{24}$	32.84	31.62	32.89	90	91.6	90	2.87	2.35
$BaTi_4O_9$(hypoth.)	3 0 −1 / 0 11 0 / 1 0 7	33	$(c)_{33}$	45.85	41.69	43.87	90	88.7	90	2.81	2.30
TiO_2(B)	1 0 6 / 0 9 0 / 3 0 0	27	$(c)_{27}$	37.32	33.62	36.49	90	89.2	90	2.84	2.32

Note. The stacking sequences, the number of layers in the sequences, the average diameters of the closest packed atoms, and the mean thickness of the closest packed layers are also given.

stices are occupied selectively by Ti, the symmetry is reduced to whatever is given as the appropriate space group in Table I. Pseudocubic cells are listed when the symmetry of a compound with c stacking is such that not one but four geometrically different pseudohexagonal unit cells are possible. The reader can apply the cubic to hexagonal transformation (see $BaTiO_3$ in Table II) in order to obtain the corresponding hexagonal cells. Not listed in Table II are the rutile related structures because they deviate too much from closest packing principles. Although the spread of individual Ba–O and O–O distances is large, the geometries of the pseudohexagonal and pseudocubic cells conform well to the closest packed arrangement. This is shown by the reasonably constant values of the average diameter of the closest packed atoms in the plane defined by the pseudocell constants a_{ph} and b_{ph} and by the remarkably constant thickness of the layers normal to c_{ph} (Table II). The pseudohexagonal cell constants have α and β values close to 90° and γ values close to 120°. The constants a_{ph} and b_{ph} agree on the average within less than 1%. The agreement are clearly worse for the pseudocubic cell constants and for the TiO_2 modifications.

In Table II the cubic and hexagonal stacking sequences of the barium titanates are listed. All six-layer titanates have the sequence ABCACB or $(hcc)_2$, while the other geometrically possible (*57*, p. 158) stacking sequence, ABCBCB or (hchhhc), does not occur.

The closest packed layers are formed by several components: by Ba and O atoms and also by additional voids in cases where two Ba atoms become next nearest neighbors in the same row of cubic closest packed atoms and the possible oxygen atom position between them is not occupied (Table III). Thus octahedral voids can be coordinated by oxygen atoms alone, or else by oxygen and by either barium and/or vacancies in the closest packing. In the barium titanates octahedral interstices coordinated by both O and Ba atoms are never occupied by Ti atoms. Neither are interstices between five O atoms and one va-

TABLE III

NUMBERS OF PACKED ATOMS IN THE PACKINGS OF THE VARIOUS BARIUM TITANATES: Ba, OXYGEN, AND VOIDS (□)

Compound	Packed atoms				Octahedral interstices		
	Ba	O	□	PA = O_c	60	Ti	□
$Ba_4(Ti,Pt)_2PtO_{10}$	16	40	8	64	12	12	0
$Ba(Ti,Pt)O_3$	6	18	0	24	6	6	0
$BaTiO_3$	1	3	0	4	1	1	0
$BaTi_2O_5$	6	30	0	36	12	12	0
$Ba_6Ti_{17}O_{40}$	24	160	8	192	72	68	4
$Ba_2Ti_{5.5}O_{13}$	4	26	2	32	12	12	0
$Ba_2Ti_2^{3+}Ti_4^{4+}O_{13}$	4	26	2	32	12	12	0
$Ba_4Ti_{10}Al_2O_{27}$	16	108	4	128	52	48	4
$Ba_4Ti_{13}O_{30}$	16	120	8	144	52	52	0
$BaTi_4O_9$(hypoth.)	2	18	2	22	8	8	0
$Ba_2Ti_9O_{20}$	8	80	2	90	43	36	7
$Ba_2Ti_{9.25}Li_3O_{22}$	4	44	0	48	28	28	0
$BaTi_5O_{11}$	4	44	0	48	26	20	6
$BaTi_6O_{13}$	2	26	0	28	17	12	5
$BaTi_6^{4+}Ti_2^{3+}O_{16}$	1	16	1	18	10	8	2
$BaTi_6Al_2O_{16}$	1	16	1	18	10	8	2
TiO_2-II	0	8	0	8	8	4	4
Rutile	0	4	0	4	4	2	2
Brookite	0	16	0	16	16	8	8
Anatase	0	8	0	8	8	4	4
TiO_2(B)	0	16	2	18	8	8	0

Note. Their sums (PA) are equal to the numbers of octahedral interstices available. The number of those coordinated by six oxygen atoms each is given (*60*), as well as the numbers of those occupied by titanium or other octahedral cations (Ti) and those remaining vacant (□).

cancy ever populated by Ti. Six-coordinated octahedral interstices are usually occupied in such a way that shared octahedral faces are avoided. Whenever unoccupied octahedra of O atoms are observed in the barium titanates, they are face sharing with neighboring Ti-occupied coordination octahedra.

The orientation of the closest packed layers can usually be derived from the morphology of the crystals or from the diffraction pattern, and yields substantial structural information, which can be used to predict large parts of the crystal structure. In the case of $Ba_2Ti_{9.25}Li_3O_{22}$, for example, the lattice constants $a = 5.81$ (2 × 2.9), $b = 9.93$ (4 × 2.5), and $c = 14.02$ (6 × 2.34) Å led to the assumption that the unit cell contained six closest packed layers perpendicular to c with four rows of two atoms each parallel to a in each layer. Because of the relatively short lattice constant a in connection with symmetry restrictions in space group *Pmcn*, the four barium atom positions in four different but symmetrically equivalent layers could easily be determined and so could the positions of all oxygen atoms in these layers. This information was sufficient to solve the structure (*32*).

Tunnel Structures (Wadsley–Andersson Phases)

$BaTi_2O_5$, $Ba_2Ti_2^{3+}Ti_4^{4+}O_{13}$, $Ba_2Ti_{5.5}O_{13}$, $BaTi_4O_9$, and TiO_2(B) belong to those compounds which all have a short cell constant of about 4 Å. This distance corresponds to the long diagonal of a TiO_6 octahedron. The structures contain infinite zig-zag bands of edge-sharing TiO_6 octahedra two or more octahedra wide. The bands are oriented parallel to the direction of the 4-Å cell edge and therefore the compounds often crystallize as needles parallel to this direction. Individual bands share common corners and in between are tunnels parallel to the bands and the short axis. These tunnels are occupied by larger cations, mostly alkali and alkali earth ions. The width of the tunnels depends on the number of octahedra in an octahedral band.

In the structure of $BaTi_4O_9$ (Fig. 10) the tunnels accommodate the Ba atoms in a pentagonal prismatic coordination. In the hypothetical $BaTi_4O_9$ structure the tunnels are two octahedra wide (Fig. 11); in $Ba_2Ti_{5.5}O_{13}$ (Fig. 12) they are three octahedra wide, as are the bands. When looking 10° off the b axis direction in $Ba_2Ti_{5.5}O_{13}$ (Fig. 13) the bands formed by the octahedra parallel to that axis become clearly recognizable. In the view parallel to the c direction, both the bands parallel to b and the short

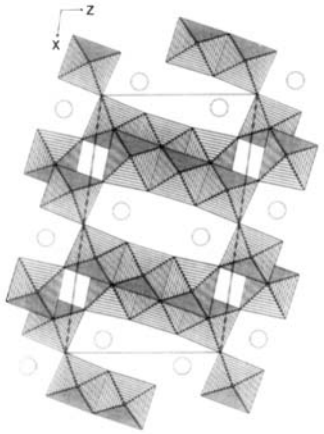

FIG. 12. Projection of $Ba_2Ti_{5.5}O_{13}$ parallel to [010] emphasizing its tunnel structure aspect. The 4.0-Å unit cell length is parallel to the direction of the view.

rutile-type octahedral chains (see below) normal to it can be seen (Fig. 14).

This type of tunnel structure is also formed by many alkali titanates and related compounds. Examples are $Na_2Ti_6O_{13}$ (*58*), $Na_2Ti_3O_7$ (*59*), KTi_3NbO_9 (*60*), $Na_xTi_4O_8$ (*61*), and the polymorph of TiO_2 known as TiO_2(B) (*25*). These compounds have often been referred to as Wadsley–Andersson phases.

Except for $BaTi_4O_9$ all the compounds

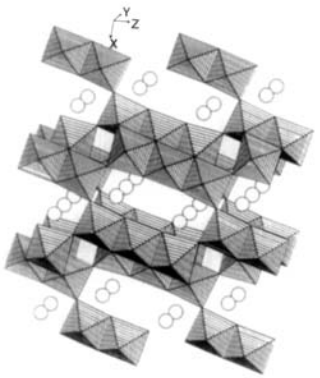

FIG. 13. Projection of $Ba_2Ti_{5.5}O_{13}$ 10° off the [010] direction. The bands of octahedra parallel to the 4.0-Å cell are apparent. Also visible are the shared edge rutile-type chains running from left to right and having a length of three octahedra.

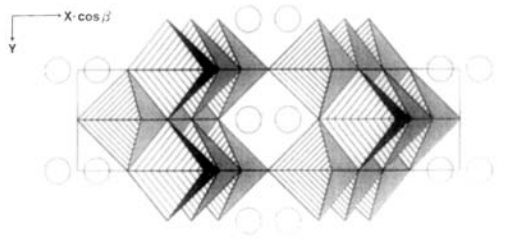

FIG. 14. Projection of $Ba_2Ti_{5.5}O_{13}$ parallel to the *c* direction, that is nearly parallel to the short rutile-type chains.

classified as Wadsley–Andersson phases in Table I can also be described as cubic closest packed arrangements of O and Ba atoms (Table II). Another way to view them is as derivatives of a hypothetical TiO in the NaCl type. By replacing an O atom $\frac{1}{2}, \frac{1}{2}, \frac{1}{2}$ in the center of the unit cell by a Ba atom, all Ti atoms except those at 0, 0, 0 would then become neighbors of the central Ba, and therefore they have to be removed. Thus we have obtained the perovskite-type cubic $BaTiO_3$ structure, which can be viewed as the simplest Wadsley–Andersson-type barium titanate. Corresponding replacements of O by Ba atoms with the consequent removal of Ti atoms in more complicated patterns and in different ratios results in the other barium titanate tunnel structures. In the same way anatase can be viewed as a NaCl type in which half the octahedral sites remain unoccupied in an ordered pattern (*57*, p. 170).

Rutile-Related 3.0-Å Phases

Rutile and the NiAs type are related as anatase and the NaCl type are. Removal of half of the cation positions in the NiAs structure in an ordered way gives an arrangement with the topology of the rutile type (Fig. 15; (*57*, p. 169). In the NiAs type the anions are hexagonally closest packed and therefore each As is surrounded by 12 As neighbors in a polyhedron of hexagonal symmetry. Thus there is only one direction

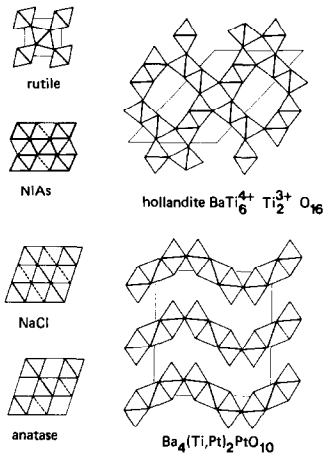

FIG. 15. Views strictly parallel the infinitely extended rutile-type chains in anatase, NaCl, NiAs, rutile, hollandite-type $BaTi_6^{4+}Ti_2^{3+}O_{16}$, and $Ba_4(Ti,Pt)_2PtO_{10}$. The latter three structures each have *two* directions in which almost closest packed, but not completely plane layers are situated at right angles to each other.

in which closest packed planes exist, while in a cubic closest packing there are four such planes (normal to [111]). In the rutile type the coordination octahedra around the Ti atoms are slightly rotated relative to the NiAs type in such a way that now there are two planes (normal to [100] and to [010]) in which the packing atoms are approximately closest packed. However, these planes are corrugated. In addition the anion packing is no longer closest packed in three dimensions, because now each anion has only 11 neighbors. This rutile packing fills only 72% of space as described by Baur (*17*).

The view of the rutile type in Fig. 15 is parallel to the *c* direction. We are looking sideways at an octahedron along one of its twofold axes. The topmost edge of the octahedron is the edge shared with a neighboring octahedron (depicted by the short diagonal of the rhomb outlining the octahedron). The coordination octahedra form chains with a repeat period of 3.0 Å parallel to the *c* direction. This type of chain can be considered the building block of a whole series of structures, such as the ramsdellites, hollandites and psilomelanes (*57*, p. 219) but also $CaTi_2O_4$, $CaFe_3O_5$, $CaFe_4O_6$, and $CaFe_5O_7$ (*62*). In many of them the rutile-type chains are fused into double rutile chains, where the neighboring chain is offset by half a repeat period in the chain direction and each octahedron shares two edges with octahedra from the neighboring chain (see hollandite, Fig. 15). The hollandite structure can be viewed as built of corner-sharing double rutile chains. The 3.0-Å structures are also tunnel structures as the example of hollandite shows. In $BaTi_6^{4+}Ti_2^{3+}O_{16}$ and in $BaTi_6Al_2O_{16}$ the tunnels accommodate the Ba atoms. The planes (001) and $(\bar{1}02)$ contain in this case the corrugated closest packed planes at right angles to each other.

In $Ba_4(Ti,Pt)_2PtO_{10}$ the *a* cell edge is 5.78 Å, or approximately twice the length of the *c* edge in rutile. Chains of octahedra extend parallel to the *a* direction, but every other octahedron is vacant. The main similarity to the rutile type is that here again one can observe two corrugated, essentially closest packed planes at right angles to each other. They are located in the planes normal to $[0\bar{1}1]$ and to [011].

Because of the intersecting corrugated close packed planes rutile, hollandite, $Ba_4(Ti,Pt)_2PtO_{10}$, and similar structures cannot be considered as closest packed. While one can give stacking sequences for these structures, it has to be understood that they cannot conform in their details to the closest packing principles as they are shown by other barium titanates.

Since several of the closest packed barium titanates have short chains of octahedra with shared edges as in the rutile type, one can view them as related to each other. An example is $Ba_2Ti_{5.5}O_{13}$, where the rutile chains are three octahedra long (Fig. 14). Fallon and Gatehouse (*63*) have pointed out that in $Ba_2Ti_9O_{20}$ there are actually hollandite-type clusters with four double

rutile chains extending for three repeat periods.

Conclusion

In Fig. 16 the ratios Ba/PA versus Ti/PA are plotted for the barium titanates, where the values of Ba, Ti and PA (total of the packed atoms) are from Table III. The value of Ti includes occupation of the octahedral interstice by Ti^{3+}, Al, or Pt, but not by Li. As the fraction of the packed sites occupied by Ba increases the value of Ti must decrease, because fewer and fewer octahedral coordination sites are surrounded solely by oxygen atoms. The line on the plot is not a regression line, but instead connects the anatase point (Ba/PA = 0.0; Ti/PA = 0.5) with the point for $BaTiO_3$ (0.25; 0.25). Whenever a point representing a barium titanate compound is not located exactly on the line, either the structure contains vacant positions in the closest packing, or possible octahedral positions are vacant in order to avoid the sharing of more than one octahedral face. More than one common face is only found in cases where atoms other than Ti also occupy octahedral sites, as in $Ba_4(Ti,Pt)_2PtO_{10}$.

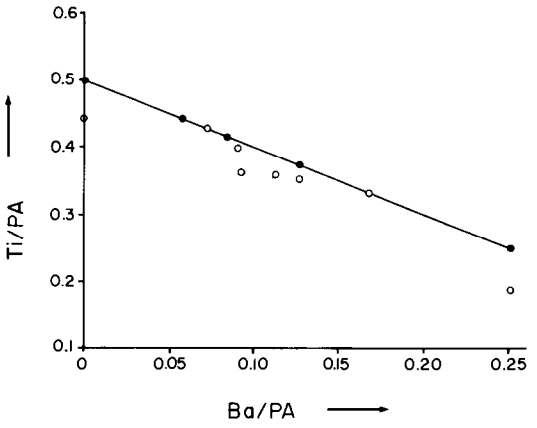

FIG. 16. Plot of Ti/PA versus Ba/PA for the barium titanates. The line connects points (0.0, 0.5) and (0.25, 0.25) with each other. It is not a regression line.

Closest packed barium titanates are only found in the range of Ba/PA from 0.0 to 0.25. At higher values there are insufficient numbers of O atoms available to supply 11 or 12 neighbors around each Ba atom. Therefore a compound such as Ba_2TiO_4 (*6*) crystallizes in a structure in which Ba is 8-coordinated, while Ti is 4-coordinated by oxygen. If it were closest packed its Ba/PA value would be 0.333. An extreme case would be a BaO structure with both Ba and O in 12 coordination, which is impossible because the topology would not allow twelve anions around a cation in an *AB* compound at the same time that twelve cations surround each anion.

Other tetravalent transition elements besides Ti form compounds with barium and oxygen. These include Ni, Cr, Mn, and Ru ($BaNiO_3$ (*37*), $BaCrO_3$ (*38*), $BaMnO_3$ (*64*) and $BaRuO_3$ (*65*)). For some of these compounds a surprisingly large number of polytypes has been described (four are known for $BaCrO_3$ (*38*); see also (*57*, p. 580)). Their compositions are always $BaXO_3$ and all are based on hexagonal closest packings with frequent sharing of octahedral faces. However, the variation in the different Ba : *X* ratios encountered in the barium titanate system is unknown here. The complicated stoichiometries of the barium titanates, together with the fact that most of them crystallize in structures derived from involved closest packings result in crystalline arrangements which are far removed from Pauling's (*66*) parsimony principle. When we use the parsimony index I_t ($=(t-e)/t$) as defined by Baur *et al.* (*67*), where t is the number of topologically distinct atomic species in the asymmetric unit, and e is the number of different chemical elements in the compound, the typical value of I_t for the $BaXO_3$ types is zero. For the complicated barium titanates the values range between 0.57 ($BaTi_5O_{11}$) and 0.9 ($BaTi_9O_{20}$). That means that they are among the most lavish inorganic structures known so far.

We make the point that even a group of compounds with seemingly unrelated stoichiometries such as the barium titanates can be described using one simple structural principle. Of the three approaches applied here, the one useful for the largest number of compounds is the closest packing principle.

Acknowledgments

We thank the University Computer Centers at Mainz and Illinois for computer time, M. Schmicking for the photographs, R. X. Fischer for making the plotting program STRUPLO available to us, and R. X. Fischer and S. Roy for reading the manuscript. Support by the National Science Foundation (Solid State Chemistry Grant DMR-80 19017 (W.H.B.)) and by NATO (Research Grant 005.82 to W.H.B. and E.T.) is gratefully acknowledged.

References

1. W. O. Statton, *J. Chem. Phys.* **19,** 33 (1951).
2. D. E. Rase and R. Roy, *J. Amer. Ceram. Soc.* **38,** 102 (1955).
3. T. Negas, R. S. Roth, H. S. Parker, and D. Minor, *J. Solid State Chem.* **9,** 297 (1974).
4. H. M. O'Bryan and J. Thomson, *J. Amer. Ceram. Soc.* **57,** 522 (1974).
5. E. Tillmanns, W. Hofmeister, and W. H. Baur, *J. Amer. Ceram. Soc.* **66,** 268 (1983).
6. J. A. Bland, *Acta Crystallogr.* **14,** 875 (1961).
7. K. K. Wu and I. D. Brown, *Acta Crystallogr. B* **29,** 2009 (1973).
8. H. D. Megaw, *Proc. R. Soc. London Ser. A* **189,** 261 (1947).
9. R. D. Burbank and H. T. Evans, Jr., *Acta Crystallogr.* **1,** 330 (1948).
10. R. Fischer and E. Tillmanns, *Z. Kristallogr.* **157,** 69 (1981).
11. E. Tillmanns and W. H. Baur, *Acta Crystallogr. B* **26,** 1645 (1970).
12. W. Hofmeister, E. Tillmanns, and W. H. Baur, *Acta Crystallogr. C* **40,** 1510 (1984).
13. E. Tillmanns, *Cryst. Struct. Commun.* **11,** 2087 (1982).
14. K. Lukaszewicz, *Rocz. Chem.* **31,** 1111 (1957).
15. D. H. Templeton and C. H. Dauben, *J. Chem. Phys.* **32,** 1515 (1960).
16. W. H. Baur and A. A. Khan, *Acta Crystallogr. B* **27,** 2133 (1971).
17. W. H. Baur, *Mater. Res. Bull.* **16,** 339 (1981).
18. E. Tillmanns, *Acta Crystallogr. B* **30,** 2894 (1974).
19. E. Tillmanns, *Acta Crystallogr.* **25,** 1444 (1969).
20. E. Tillmanns, *Cryst. Struct. Commun.* **1,** 1 (1972).
21. W. H. Baur, *Acta Crystallogr.* **14,** 214 (1961).
22. E. P. Meagher and G. A. Lager, *Canad. Mineral.* **17,** 77 (1979).
23. M. Horn, C. F. Schwerdtfeger, and E. P. Meagher, *Z. Kristallogr.* **136,** 273 (1972).
24. P. Y. Simons and F. Dachille, *Acta Crystallogr.* **23,** 334 (1967).
25. R. Marchand, L. Brohan, and M. Tournox, *Mater. Res. Bull.* **15,** 1129 (1980).
26. F. Theobald, R. Cabala, and J. Bernard, *J. Solid State Chem.* **17,** 431 (1976).
27. L. Bourgeois, *Bull. Soc. Mineral* **9,** 244 (1886).
28. T. Kubo and K. Shinriki, *Kogyo Kagaku Zasshi* **54,** 268 (1951)
29. K. Kato, I. Kawada, and K. Muramatsu, *Acta Crystallogr. B* **30,** 1634 (1974).
30. G. H. Jonker and W. Kwestroo, *J. Amer. Ceram. Soc.* **41,** 390 (1985).
31. W. Hofmeister and E. Tillmanns, *Acta Crystallogr. B* **35,** 1590 (1979).
32. E. Tillmanns and I. Wendt, *Z. Kristallogr.* **144,** 16 (1976).
33. W. H. Baur, E. Tillmanns, and W. Hofmeister, W., *Cryst. Struct. Commun.* **11,** 2021 (1982).
34. J. Schmachtel and Hk. Müller-Buschbaum, *Z. Naturforsch. B* **35,** 332 (1980).
35. J. Schmachtel and Hk. Müller-Buschbaum, *Z. Anorg. Allg. Chem.* 472, 89 (1981).
36. E. Tillmanns, *in* "Handbook of Geochemistry" (K. H. Wedepohl, Ed.), Vol. II, Springer-Verlag, Berlin (1972).
37. Y. Takeda, F. Kanamaru, M. Shimada, and M. Koizumi, *Acta Crystallogr. B* **32,** 2464 (1976).
38. B. L. Chamberland, *J. Solid State Chem.* **43,** 309 (1982).
39. K. B. Schwartz and C. T. Prewitt, *J. Phys. Chem. Solids* **44,** 1 (1984).
40. R. D. Shannon, *Acta Crystallogr. A* **32,** 751 (1976).
41. H. D. Megaw, *Acta Crystallogr.* **15,** 972 (1962).
42. M. Mayer and G. Perez, *Rev. Chim. Mineral.* **13,** 237 (1976).
43. V. P. Balko and V. V. Bakakin, *J. Struct. Chem.* **16,** 773 (1976).
44. H. Cid-Dresdner and M. J. Buerger, *Z. Kristallogr.* **117,** 411 (1962).
45. W. R. Robinson, *J. Solid State Chem.* **9,** 255 (1974).
46. S.-H. Hong and S. Åsbrink, *Acta Crystallogr. B* **38,** 2570 (1982).
47. M. Marezio, D. B. McWhan, P. D. Dernier,

AND J. P. REMEIKA, *J. Solid State Chem.* **6,** 213 (1973).
48. M. MAREZIO, D. TRANQUI, S. LAKLIS, AND L. SCHLENKER, *Phys. Rev. B* **16,** 2811 (1977).
49. Y. LEPAGE AND P. STROBEL, *J. Solid State Chem.* **43,** 314 (1982).
50. Y. LEPAGE AND P. STROBEL, *J. Solid State Chem.* **44,** 272 (1982).
51. L. PAULING, "The Nature of the Chemical Bond" 3rd ed., Cornell Univ. Press, Ithaca, N.Y. (1960).
52. W. H. BAUR, (1970). *Trans. Amer. Crystallogr. Assoc.* **6,** 129 (1970).
53. W. H. BAUR, *in* "Structure and Bonding in Crystals", (M. O.'Keeffee and A. Navrotsky, Eds.), Vol. 11, p. 31, Academic Press, New York (1981).
54. I. D. BROWN AND R. D. SHANNON, *Acta Crystallogr. A* **29,** 266 (1973).
55. I. D. BROWN AND K. K. WU, *Acta Crystallogr. B.* **32,** 1957 (1976).
56. M. HERVIEU, G. DESGARDIN, AND B. RAVEAU, *J. Solid State Chem.* **30,** 375 (1979).
57. A. F. WELLS, "Structural Inorganic Chemistry," 5th ed., Oxford Univ. Press, London (1984).
58. S. ANDERSSON AND A. D. WADSLEY, *Acta Crystallogr.* **15,** 194 (1962).
59. S. ANDERSSON AND A. D. WADSLEY, *Acta Crystallogr.* **14,** 1245 (1961).
60. A. D. WADSLEY, *Acta Crystallogr.* **17,** 623 (1964).
61. S. ANDERSSON AND A. D. WADSLEY, *Acta Crystallogr.* **15,** 201 (1962).
62. W. H. BAUR, *J. Solid State Chem.* **43,** 222 (1982).
63. G. D. FALLON AND B. M. GATEHOUSE, *J. Solid State Chem.* **49,** 59 (1983).
64. A. D. POTOFF, B. L. CHAMBERLAND, AND L. KATZ, *J. Solid State Chem.* **8,** 234 (1973).
65. P. C. DONOHUE, L. KATZ AND R. WARD, *Inorg. Chem.* **4,** 306 (1965).
66. L. PAULING, *J. Amer. Chem. Soc.* **51,** 1010 (1929).
67. W. H. BAUR, E. TILLMANNS, AND W. HOFMEISTER, *Acta Crystallogr. B* **39,** 669 (1983).
68. J. SCHMACHTEL AND HK. MÜLLER-BUSCHBAUM, *Z. Anorg. Allg. Chem.* **435,** 243 (1977).
69. W. SINCLAIR, G. M. MCLAUGHLIN, AND A. E. RINGWOOD *Acta Crystallogr. B* **36,** 2913 (1980).